Acta Cryst. (1997). D53, 419–425

Structure of Crystal Form IX of Bovine Pancreatic Ribonuclease A

MEI H. DUNG AND JEFFREY A. BELL

Department of Chemistry and Center for Biophysics, Rensselaer Polytechnic Institute, Troy, NY 12180, USA. E-mail: bell@xray.chem.rpi.edu

(Received 13 September 1996; accepted 21 January 1997)

Abstract

The X-ray structure of crystal form IX of bovine pancreatic ribonuclease A (space group $P2_12_12_1$) is reported at 1.6 Å resolution. The structure was refined to an R factor of 15.0% and includes coordinates for two sulfate ions, four methanol molecules and 82 waters. The structure could be superimposed on the highest resolution crystal structure of bovine pancreatic ribonuclease available (in space group $P2_1$) with an r.m.s. difference in main-chain atomic positions of 0.51 Å. Most of the larger differences between the two structures could be related to crystal lattice contacts. Superposition of the new structure with eight other structures of ribonuclease in six crystal forms resulted in an r.m.s. deviation from the average structure of 0.43 Å for all main-chain atoms. This similarity among structures exists in spite of the fact that all nine molecules are in different crystal environments.

1. Introduction

Bovine pancreatic ribonuclease crystallizes in at least 38 different crystal modifications (King, Magdoff, Adelman & Harker, 1956; King, Bello, Pignataro & Harker, 1962). One of these crystal forms, modification IX of King, Bello, Pignataro & Harker (1962), has an unusual property that sets it apart from most other reported protein crystals in that these crystals diffract at high resolution without chemical cross-linking when severely dehydrated, whether in dry air or when solvated by many, but not all, organic liquids (King *et al.*, 1962; J. A. Bell, unpublished results).

Exploration of the structure of a dehydrated protein could provide insight into the effects of water on protein structure; into the consequences of dehydration of proteins during freeze-drying in bioprocessing; and into the properties of proteins in non-aqueous liquid environments. A preliminary report (Bell, 1997) briefly describes some of the effects of severe dehydration on the structure of this crystal form of bovine pancreatic ribonuclease.

We report here the refined structure of crystal form IX of bovine pancreatic ribonuclease determined under fully solvated conditions. Of all the crystal forms of bovine pancreatic ribonuclease with known X-ray structures, only the structure of the $P2_1$ crystal form has been based on data collected to higher resolution (Borkakoti, Moss & Palmer, 1982; Campbell & Petsko, 1987; Wlodawer, Svensson, Sjölin & Gilliland, 1988; Howlin, Moss & Harris, 1989).

2. Methods

Crystals of bovine pancreatic ribonuclease were grown by modification of the original procedure (King *et al.*, 1956, 1962). Bovine pancreatic ribonuclease A (Sigma) was dissolved in ultra-pure water (Barnstead milliQ), producing a solution of approximately pH 4.5. Crystals were grown by the batch method in glass vials at room temperature using methanol as a precipitant. The best crystals were produced at protein concentrations near 15 mg ml^{-1}, and methanol concentrations near 58%(*v*/*v*). Such conditions occasionally produced samples of the needle-shaped crystals with dimensions up to 0.14 × 0.14 mm in cross section, and up to 1.0 mm in length. Crystals were mounted in glass capillaries containing 60% aqueous methanol at the ends of the tubes.

Data collection was carried out at 292 K, using a Rigaku R-AXIS image-plate detector mounted on a RU-200 rotating-anode X-ray generator with graphite monochromator.

Data-collection and processing statistics are summarized in Table 1. Reflections with $I/\sigma(I) > 2$ were used to produce the final 1.6 Å data set. Four crystals were used to minimize X-ray damage and to help average out absorption effects, although a single crystal might have sufficed. On average, each reflection was measured more than six times.

The initial model structure used for molecular replacement was that of ribonuclease A in space group $P2_1$ with Protein Data Bank identifier 3RN3 (Howlin *et al.*, 1989). Molecular replacement was accomplished using the *MERLOT* program package (Fitzgerald, 1988).

The restrained least-squares program *TNT* (Tronrud, Ten Eyck & Matthews, 1987) was used for structural refinement. The model obtained from molecular replacement was subjected first to rigid-body refinement, followed by 30 sets of alternating cycles of positional and temperature-factor refinement, essentially as previously described (Bell *et al.*, 1991). All data from 10

Table 1. *Data-collection statistics*

Space group	$P2_12_12_1$
Cell dimensions (Å)	45.9, 44.8, 52.9
Number of crystals	4
Number of frames	98
Crystal-to-detector distance (mm)	60
Average mosaicity (°)	0.25
Oscillation angle (°)	3.0
Exposure time (min)	10
Total observations	76694
Independent reflections	12318
R_{merge} (intensity) (%)	8.3
Resolution limit (Å)	1.6

Shell (Å)	Average $I/\sigma(I)$	Percent complete $I/\sigma(I) > 2$
∞–15	13.45	79
15–10	13.79	93
10–7	12.19	90
7–4	11.97	96
4–3	10.15	95
3–2.6	7.68	96
2.6–2.2	6.34	94
2.2–2.0	5.28	90
2.0–1.8	4.44	85
1.8–1.6	4.22	61
Overall	6.36	82

to 1.6 Å was used in the final refinement. Temperature factors were not restrained. Occupancy was not refined because of insufficiently high resolution. In between each set of refinement cycles, difference maps and omit maps (Bhat & Cohen, 1984) were examined manually using the program *FRODO* (Jones, 1978) on an Evans & Sutherland PS390. Side chains with high temperature factors or associated with significant difference map features were deleted for the subsequent set of refinement cycles and then manually placed in observed electron density. Solvent molecules were added gradually in the refinement process, and only after the protein structure was determined.

Methanol molecules were tentatively identified on the basis of cylindrical electron density in the solvent, and low to moderate temperature factors for both atoms after unrestrained temperature factor refinement. All solvent molecules were included in the final model only if their omission resulted in a difference feature of at least 4σ and if no short contacts were observed with protein or other solvent atoms.

Sulfate ions were identified without reference to other ribonuclease structures, on the basis of tetrahedral density shape, and confirmed by the presence of positive difference peaks within approximately 1.5 Å of the O atom if a water molecule was refined in place of the sulfate. Since electron density alone could not be used to distinguish sulfate ions from phosphate ions, anion chromatography (Quantitative Technologies, Inc.) was used to established the presence of sulfate and not phosphate in protein ultrafiltrate produced using an Centricon 10 microconcentrator (Amicon). Presumably the presence of sulfate is the result of the purification process used in the commercial preparation.

Table 2 summarizes refinement statistics. Stereochemical restraints were from the *TNT* Protgeo library. No chiral center had the wrong handedness.

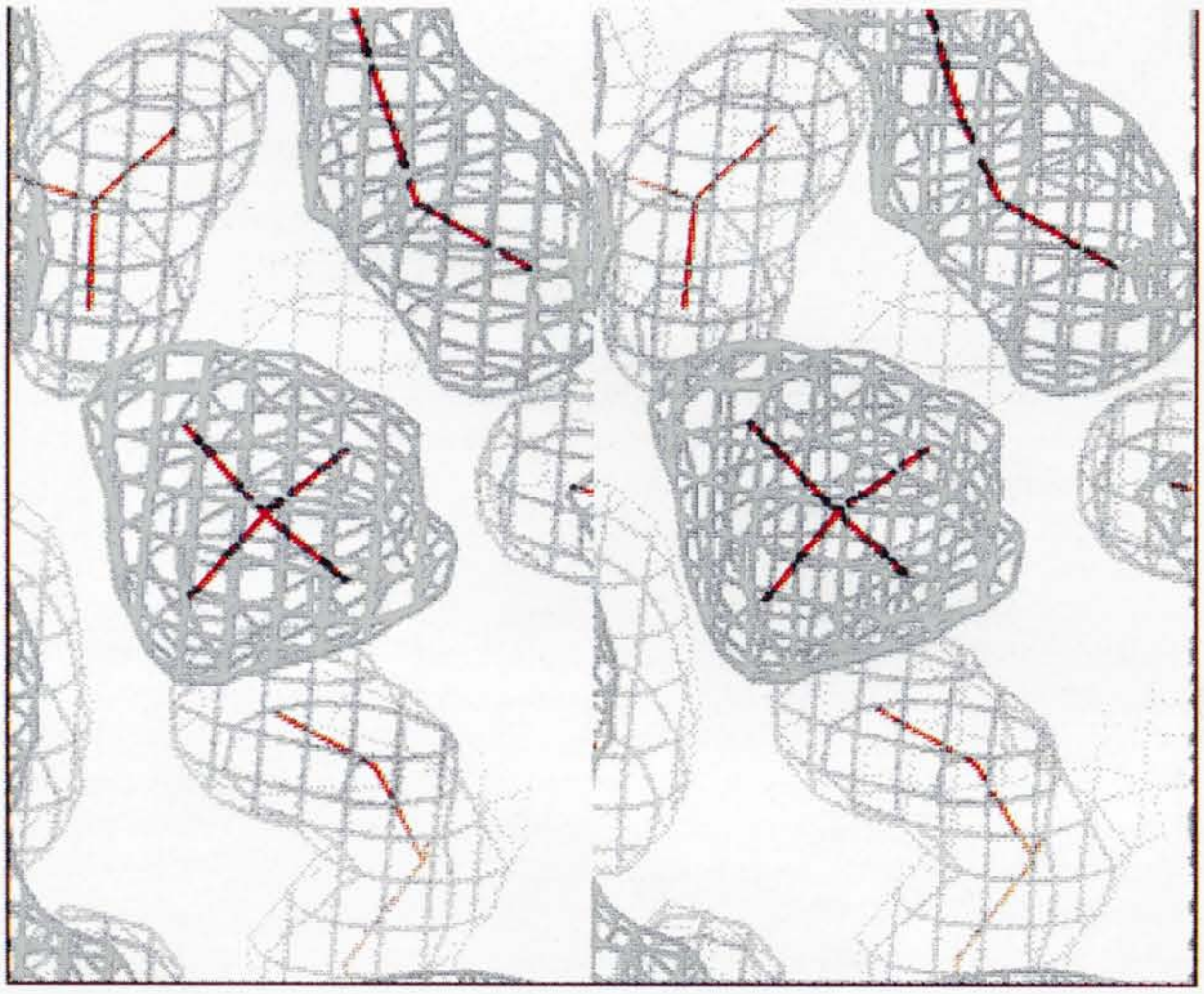

Fig. 1. Stereo pair of the electron-density map ($2F_{obs} - F_{calc}$) near sulfate ion 150. Side chains visible in this figure are (starting from the uper left, and proceeding clockwise): Asn34, Lys37, Ser22 and Ser23. The hydroxyl O atom of Ser22 is just visible at the right edge of this figure. This view places the observer near Ser50 (not shown). Atomic coordinates for the sulfate ion were excluded in the phase calculation. Contour level is 1.2σ.

Multiple structure superposition was performed according to the method of Diamond (1992), as implemented in the *CCP*4 package (Collaborative Computational Project, Number 4, 1994). Pairs of structures were compared using the function in *TNT* (Tronrud *et al.*, 1987) which implements the superposition method of Kabsch (1978).

3. Results

The molecular replacement procedure was very straightforward. Only one peak above 65% of the maximum peak height was found from the Lattman rotation function (Lattman & Love, 1972). This rotation occurred at $\alpha = 157.5$, $\beta = 90.0$, $\gamma = 255.0°$. Information from the packing function (Hendrickson & Ward, 1976) at this rotation was sufficient to place the known structure in this crystal form at [0.040, 0.20, 0.090].

The electron density is very clear for all main-chain atoms, except for Lys1. Most side chains were also easily placed in unambiguous electron density. Electron density associated with certain side chains was difficult to model as a single conformation of that side chain: Lys1, Lys7, Ser21, Asn24, Gln28, Lys31, Leu51, Arg 85, Lys91, Asn94, Lys98, Gln103 and Asn113. The single conformation suggested for each of these side chains is consistent with the weak electron density observed, and is probably one of many conformations that each of these side chains actually adopts.

The final model contains coordinates for all 951 non-H atoms in the protein, plus 82 water molecules, four methanol molecules and two sulfate ions. The average

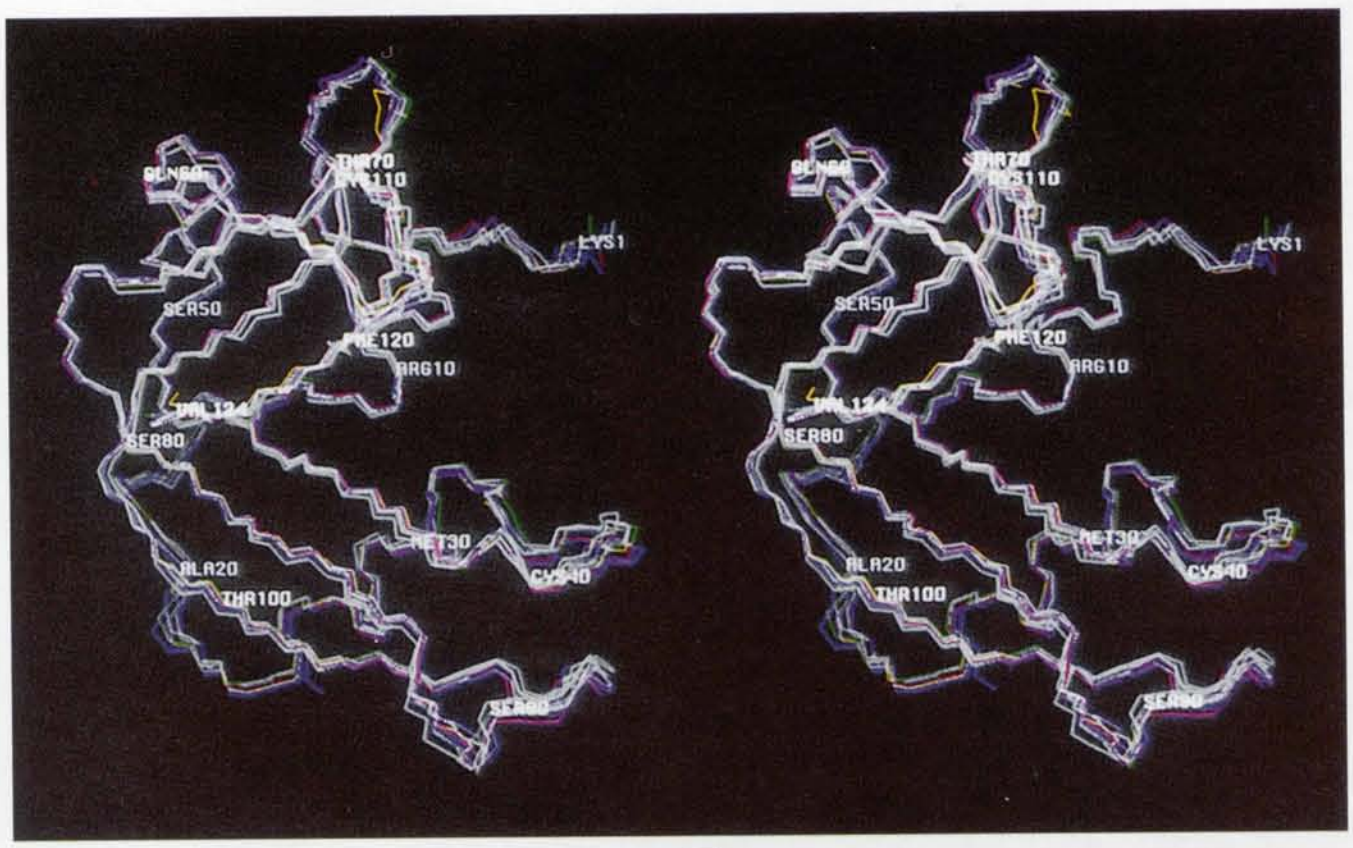

(*a*)

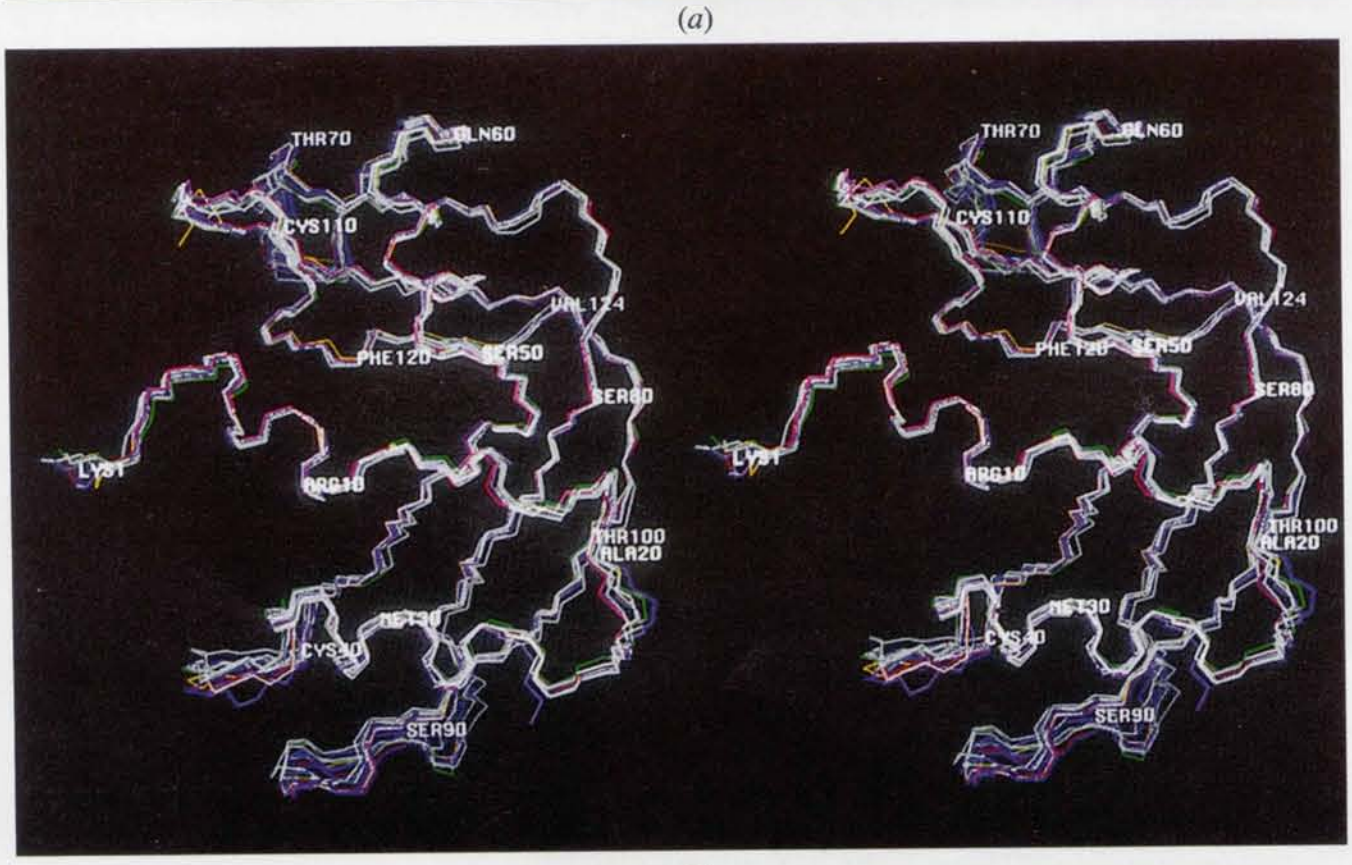

(*b*)

Fig. 2. Stereo pair of backbone tracing of the structures of nine independent molecules of ribonuclease from seven different crystal forms. The two images show the same set of structures from opposite sides of the molecule. All other structures were superimposed by linear least-squares fit to the form IX crystal structure. Color key: ribonuclease crystal form IX, blue (this work); 7RSA, purple (Wlodawer *et al.*, 1988): IRSM, green-blue (Weber, Sheriff, Ohlendorf, Finzel & Salemme, 1985); 2RNS, magenta (Kim *et al.*, 1992); 8RSA molecule A, red; 8RSA molecule *B*, red-orange (Nachman *et al.*, 1990); 4SRN, orange (deMel *et al.*, 1992); IRBB molecule *A*, cyan: IRBB molecule *B*, green (Williams, Greene & McPherson, 1987).

isotropic thermal factor for the water molecules was 34.2 Å^2 and ranged from 12.4 to 56.0 Å^2.

Each of the four methanol molecules in the solvent region fit the observed electron density much better than a single water molecule, but identification of these electron-density peaks as methanol is necessarily tentative at the resolution of this structure.

The electron density for sulfate 150 is shown in Fig. 1. Sulfate 150 is within hydrogen-bonding distance (less than 3.5 Å) of Ser50 (not shown in Fig. 1) in one molecule, Asn34 and Lys37 in a symmetry-related molecule, and Ser22 and Ser23 in a second symmetry-related molecule. The location of sulfate 150 is near the N-terminus of the helix extending from residues 50 to 60 in one molecule, and also near the N-terminus of the helix extending from residues 24 to 34 in a symmetry-related molecule.

The electron density for sulfate ion 150 is better defined than the electron density around sulfate 151 which is found in the active site. The thermal parameters for all of the atoms in sulfate 151 are higher than for the corresponding atoms in sulfate 150. These observations regarding sulfate ion 151 might be the result of greater static disorder, greater molecular dynamics or lower occupancy than sulfate 150.

The intermolecular contacts in the form IX crystals are composed of only four different interfaces generated by independent symmetry operators, and are listed in Table 3.*

Table 2. *Summary of refinement statistics*

R factor			
After molecular replacement	0.400*		
After rigid-body refinement	0.378*		
Final (10–1.6 Å)	0.150		
By resolution range (Å)			
10.0–4.32	0.13		
4.31–3.00	0.13		
2.99–2.53	0.15		
2.52–2.27	0.15		
2.26–2.08	0.17		
2.07–1.95	0.18		
1.94–1.85	0.19		
1.84–1.76	0.20		
1.75–1.69	0.21		
1.68–1.60	0.23		
Model geometry	Number	Weight	R.m.s. deviation
Bond length (Å)	983	1.0	0.010
Bond angle (°)	1321	1.5	1.93
Planar group (Å)	140	4.0	0.010
Trigonal atom planarity (Å)	28	1.5	0.016
Bad contacts (Å)	4	20	0.008
Atoms in refinement	1051		
Reflections in refinement	12318		

* Resolution range 10–3 Å.

4. Discussion

The highest resolution structure (1.26 Å) of bovine pancreatic ribonuclease available is 7RSA (Wlodawer *et al.*, 1988). Therefore, a detailed comparison of the new structure with 7RSA was performed (Figs. 2 and 3).

After superposition of main-chain atoms of 7RSA onto the corresponding form IX coordinates, the r.m.s. deviation for those atoms was 0.51 Å. The difference in atomic position between the two structures is plotted in Fig. 3 for all atoms. In general, differences of more than 1.5 Å indicated in Fig. 3 involve only side-chain atoms of surface residues. Exceptions to this observation are in the backbone atoms described in the next paragraph.

Two regions of the amino-acid sequence, residues 18–22 and residues 37–39, represent the largest main-chain differences observed (Figs. 2 and 3). Interestingly, residues in these two regions form a crystal lattice contact with one another in crystal form IX, and are involved in the coordination of sulfate ion 150 as part of that interface. The only other large main-chain conformational change involves Lys1, which is in a very different conformation in the two crystal forms, due to a rotation about the ψ backbone torsion angle.

Almost all residues that are identified by number in Fig. 3 (plus residues 38, 93, 102 and 103) are involved in lattice contacts in crystal form IX or 7RSA. Thus, almost all of the large differences in these two crystal structures could be rationalized on the basis of effects of crystal contacts.

However, five amino-acid side chains with large differences in position are not directly involved in crystal contacts: Lys7, Gln11, Lys31, Asn94 and Gln101. Lys7 and Gln11 are active-site residues, and their conformations are probably affected by the presence of sulfate 151, as mentioned below. The differences between the two structures at Lys31 and Asn94 are not easy to account for, but they do involve side chains for which clear electron density is lacking in form IX. The side chain of Gln101, which is in a solvent-exposed position in 7RSA, is partially buried in form IX. This difference cannot be attributed directly to crystal contacts. Only one set of coordinates is given for this side chain in 7RSA, and all atoms have moderate thermal parameters. In the form IX crystal structure, this side chain has low thermal parameters. Thus, this difference in position appears to be real. A related observation regarding solvent molecules is described below.

Of the 88 solvent molecules and ions identified in the form IX crystal structure, 59% have a counterpart in the solvent model for 7RSA. Solvent molecules were considered analogous if they occupied a position within 1.0 Å of each other (symmetry-related solvent included), and at least one hydrogen-bond partner was the same. The resolution was not high enough to assign partial

* Atomic coordinates and structure factors have been deposited with the Protein Data Bank, Brookhaven National Laboratory (Reference: 1BEL, R1BELSF). Free copies may be obtained through The Managing Editor, International Union of Crystallography, 5 Abbey Square, Chester CH1 2HU, England (Reference: GR0675).

Table 3. *Protein intermolecular crystal contacts*

Residues listed have at least one atom in contact with (*i.e.* within 5 Å of) an atom from a symmetry-related molecule. Each interface is the result of a single symmetry operation.

Interface	Residue Molecule 1	Residue Molecule 2	Interface	Residue Molecule 1	Residue Molecule 2
1	Ser18	Lys1	3	Lys7	Asp14
	His48	Glu2		Lys37	Ser16
	Glu49	Ala6		Asp38	Thr17
	Ser50	Glu9		Arg39	Ala19
	Ala52	Arg10			Ala20
	Asp53	Met13			Ser21
	Gln55	Asp14			Ser22
	Ala56	Ser15			Asn24
	Ser59	Ser16			Tyr25
	Gln60	Met29			Met29
	Lys61	Ser32			Arg33
	Asn62	Arg33			
	Tyr76	Asn34	4	Arg39	Ser59
	Ser77	Lys37		Pro42	Gln60
	Ser80	Leu51		Val43	Asn62
				Lys66	Gly68
2	Ala64	Thr78		Glu86	Gln69
	Lys66	Gln101		Thr87	Thr70
	Gly68	Ala102		Gly88	Asn71
		Asn103		Ser90	Gly112
		Lys104		Lys91	Asn113
					Tyr115

occupancy for water molecules as was done for 7RSA, where 189 solvent positions were identified. An exact correspondence between water models would not be expected since crystal contacts and solution constituents may well have significant effects on bound solvent. The above percentages are similar to the comparison of solvent structures found in the same crystal form of T4 lysozyme at three different ionic strengths (Bell *et al.*, 1991) and for two crystal forms of chicken lysozyme (Moult *et al.*, 1976). Comparison of three crystal forms of bovine trypsin inhibitor indicated very different sets of solvent molecules (Wlodawer, Deisenhofer & Huber, 1987; Wlodawer, Nachman & Gilliland, 1987).

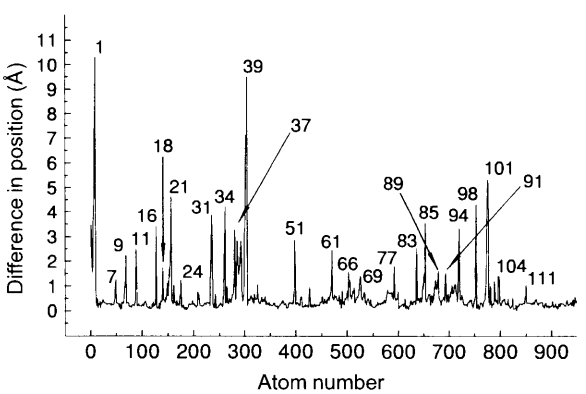

Fig. 3. Differences in position for all non-H protein atoms between form IX and 7RSA. The two structures were superimposed by main-chain atoms. Residue numbers are given above the plot. Atom numbering is according to form IX (Protein Data Bank reference 1BEL). Where more than one conformation was provided in the 7RSA coordinates, the one with the higher occupancy was used in this comparison, or the '*A*' conformation was used if both conformations had the same occupancy.

Two sulfate ions were identified in the solvent region of the electron-density map. Sulfate 150, at an intermolecular interface, was described in the *Results* section, and is the one more clearly seen in the electron density. Sulfate 150 does not seem to have a counterpart in any other crystal form of bovine pancreatic ribonuclease in the Protein Data Bank (Bernstein *et al.*, 1977; Abola, Bernstein, Bryant, Koetzle & Weng, 1987).

Sulfate ion 151 is in the active site, at a similar position to the sulfate found in Protein Data Bank coordinate sets 2RNS (Kim, Varadarajan, Wyckoff & Richards, 1992), 4SRN (deMel, Martin, Doscher & Edwards, 1992), and 3RN3 (Howlin *et al.*, 1989), associated with the side chains of residues Gln11, His12 and His119. The crystal form used to determine the structure of 3RN3 is the same crystal form as 7RSA, but 7RSA does not include a sulfate (or phosphate) at this site because care was taken to exclude such ions from the crystal (Campbell & Petsko, 1987; Wlodawer *et al.*, 1988).

The binding of methanol to bovine pancreatic ribonuclease in form IX crystals might best be compared with the acetonitrile molecules bound to cross-linked porcine pancreatic elastase crystals in neat acetonitrile (Allen *et al.*, 1996). In that crystallographic study at a slightly lower resolution, nine acetonitrile molecules were identified bound to the protein, three of them in crystal contact regions. Three of the four methanol sites in form IX crystals involve crystal contacts.

Methanol 171 appears to share a hydrogen bond with water 266, and interacts at the other end with O1 of sulfate 150, and the side chains of Lys37 and Asn52. Acetonitrile molecules 701 and 702 also interact with a sulfate ion in the elastase structure (Allen *et al.*, 1996).

Methanol 170 hydrogen bonds to the main chain of Tyr76 and the side chain of Gln60 in one molecule. The other end of methanol 170 interacts with the main-chain atoms of Ala6 and Arg10 in a symmetry-related molecule. Methanol 173 interacts with the side chain of Glu86 of one molecule and with Tyr73 of a symmetry-related molecule. No obvious parallel exists between these methanols and the acetonitriles observed in the porcine elastase structure. Two of the bound acetonitrile molecules in the elastase structure were found in the active site. Methanol 172 is in the active site in form IX crystals and it is the only methanol that does not form contacts with more than one protein molecule. Interactions occur between methanol 172 and the side chains of Arg10 and Gln11.

The location of the one molecule of *t*-butanol identified in 7RSA is not related to the location of any of the four bound methanol molecules. However, water 238 is in a very similar position as *t*-butanol 125 in 7RSA. Gln101 is close to *t*-butanol 125 in 7RSA, but it is not in a conformation that brings it close to water 238 in the form IX crystal structure. Perhaps this interaction with *t*-butanol in 7RSA explains the difference in structure at Gln101 noted above.

Active-site residues are in similar positions in 7RSA and in the form IX crystal structure. All atoms of His12 and His119 in form IX are within 0.2 Å of their position in 7RSA. Gln11 is in a very similar position in both structures, except that χ_3 is almost 180° different, *i.e.*, the O atom and the N atom of the side-chain amide are assigned in an opposite manner. For the form IX structure, this choice was dictated by the opportunity to form a hydrogen bond between Gln11 and sulfate 151 if the amide N atom were nearby. Lys7 and Lys41 are in similar positions in the two structures, with r.m.s. differences in position of 0.76 and 0.41 Å for all side-chain atoms in the respective residues. Lys7 is in a better position to interact with an active-site sulfate ion in form IX than it would be in 7RSA.

A subset was chosen of the various other known crystal structures of bovine pancreatic ribonuclease and its derivatives to determine if the conformation of ribonuclease in form IX crystals was unusual, or especially affected by the presence of sulfate 150 at a crystal contact. This subset (listed in the legend to Fig. 2) contains representatives for all of the crystal forms available from the Protein Data Bank (Bernstein *et al.*, 1977; Abola *et al.*, 1987). Where multiple determinations have been made of the same or similar crystal forms, the structure that has the highest resolution has been chosen for these comparisons. This selection process produced a set of structures similar to that employed by Crosio, Janin & Jullien (1992) in their discussion of ribonuclease crystal packing.

Fig. 2 compares the backbone tracing for each of the nine structures listed in the legend. The crystal form IX structure does not have any particular outstanding differences from all of the other structures. The differences among the structures are small except in certain coil or turn regions of the molecules. The r.m.s. difference in main-chain positions between structures is 0.65 Å. The r.m.s. main-chain difference from the average structure is 0.43 Å (Diamond, 1992). The backbone positions vary modestly, despite the fact that each structure is the result of a different crystal packing environment.

This work was supported by NIH grant GM50817. Thanks to Swagata Dasgupta, Ganesh H. Iyer and Jiancheng Xuan for programming assistance. The use of the X-ray diffraction equipment of the Macromolecular Crystallographic Core Facility of the Wadsworth Center, New York State Department of Health, Albany, NY is gratefully acknowledged.

References

Abola, E. E., Bernstein, F. C., Bryant, S. H., Koetzle, T. F. & Weng, J. (1987). *Crystallographic Databases – Information Content, Software Systems, Scientific Applications*, edited by F. H. Allen, G. Bergerhoff & R. Sievers, pp. 107–132. Bonn/Cambridge/Chester: IUCr.

Allen, K. N, Bellamacina, C. R., Ding, X., Jeffery, C. J., Mattos, C., Petsko, G. A. & Ringe, D. (1996). *J. Phys. Chem.* **100**, 2605–2611.

Bell, J. A. (1997). *Biomacromolecules: From 3-D Structure to Applications. Proceedings, 34th Hanford Symposium on Health and the Environment*, edited by R. L. Ornstein, pp. 231–238. Columbus: Battelle.

Bell, J. A., Wilson, K. P., Zhang, X.-J., Faber, H. R., Nicholson, H. & Matthews, B. W. (1991). *Proteins*, **10**, 10–21.

Bernstein, F. C., Koetzle, T. F., Williams, G. J. B., Meyer, E. F. Jr, Brice, M. D., Rodgers, J. R., Kennard, O., Shimanouchi, T. & Tasumi, M. (1977). *J. Mol. Biol.* **112**, 535–542.

Bhat, T. N. & Cohen, G. H. (1984). *J. Appl. Cryst.* **17**, 244–248.

Borkakoti, N., Moss, D. S. & Palmer, R. A. (1982). *Acta Cryst.* B**38**, 2210–2217.

Campbell, R. L. & Petsko, G. A. (1987). *Biochemistry*, **26**, 8579–8584.

Collaborative Computational Project, Number 4. (1994). *Acta Cryst.* D**50**, 760–763.

Crosio, M.-P., Janin, J. & Jullien, M. (1992). *J. Mol. Biol.* **228**, 243–251.

Diamond, R. (1992). *Protein Sci.* **1**, 1279–1287.

Fitzgerald, P. M. D. (1988). *J. Appl. Cryst.* **21**, 273–278.

Hendrickson, W. A. & Ward, K. B. (1976). *Acta Cryst.* A**32**, 778–780.

Howlin, B., Moss, D. S. & Harris, G. W. (1989). *Acta Cryst.* A**45**, 851–861.

Jones, T. A. (1978). *J. Appl. Cryst.* **11**, 268–272.

Kabsch, W. (1978). *Acta Cryst.* A**34**, 827–828.

Kim, E. E., Varadarajan, R., Wyckoff, H. W. & Richards, F. M. (1992). *Biochemistry*, **31**, 12304–12314.

King, M. V., Bello, J., Pignataro, E. H. & Harker, D. (1962). *Acta Cryst.* **15**, 144–147.
King, M. V., Magdoff, B. S., Adelman, M. B. & Harker, D. (1956). *Acta Cryst.* **9**, 460–465.
Lattman, E. E. & Love, W. E. (1972). *Acta Cryst.* B**26**, 1854–1857.
deMel, V. S. J., Martin, P. D., Doscher, M. S. & Edwards, B. F. P. (1992). *J. Biol. Chem.* **267**, 247–256.
Moult, J., Yonath, A., Traub, W., Smilansky, A., Pojarny, A., Rabinovich, D. & Saya, A. (1976). *J. Mol. Biol.* **100**, 179–195.
Nachman, J., Miller, M., Gilliland, G. L., Carty, R., Pincus, M. & Wlodawer, A. (1990). *Biochemistry*, **29**, 928–937.
Tronrud, D. E., Ten Eyck, L. F. & Matthews, B. W. (1987). *Acta Cryst.* A**43**, 489–501.
Weber, P. C., Sheriff, S., Ohlendorf, D. H., Finzel, B. C. & Salemme, F. R. (1985). *Proc. Natl Acad. Sci. USA*, **82**, 8473–8477.
Williams, R. L., Greene, S. M. & McPherson, A. (1987). *J. Biol. Chem.* **262**, 16020–16030.
Wlodawer, A., Deisenhofer, J. & Huber, R. (1987). *J. Mol. Biol.* **193**, 145–156.
Wlodawer, A., Nachman, J. & Gilliland, G. L. (1987). *J. Mol. Biol.* **198**, 469–480.
Wlodawer, A., Svensson, L. A., Sjölin, L. & Gilliland, G. L. (1988). *Biochemistry*, **27**, 2705–2717.